Generating Triple Crystalline Superstructures in Melt Miscible PEO-*b*-PCL-*b*-PLLA Triblock Terpolymers by Controlling Thermal History and Sequential Crystallization

Jordana K. Palacios, Guoming Liu, Dujin Wang, Nikos Hadjichristidis and Alejandro J. Müller**

(Dedicated to the memory of Prof. Dr. Reimund Stadler)

Dr. J. K. Palacios
POLYMAT and Polymer Science and Technology Department, Faculty of Chemistry, University of the Basque Country UPV/EHU, Paseo Manuel de Lardizabal 3, 20018 Donostia-San Sebastián, Spain.

Dr. Guoming Liu
Beijing National Laboratory for Molecular Sciences, CAS Research/Education Center for Excellence in Molecular Sciences, CAS Key Laboratory of Engineering Plastics, Institute of Chemistry, Chinese Academy of Sciences, Beijing, 100190, China.

Prof. Dujin Wang
Beijing National Laboratory for Molecular Sciences, CAS Research/Education Center for Excellence in Molecular Sciences, CAS Key Laboratory of Engineering Plastics, Institute of Chemistry, Chinese Academy of Sciences, Beijing, 100190, China.

Prof. N. Hadjichristidis
King Abdullah University of Science and Technology (KAUST), Physical Sciences and Engineering Division, KAUST Catalysis Center, Thuwal, Saudi Arabia.
E-mail: nikolaos.hadjichristidis@kaust.edu.sa

Prof. A. J. Müller
POLYMAT and Polymer Science and Technology Department, Faculty of Chemistry, University of the Basque Country UPV/EHU, Paseo Manuel de Lardizabal 3, 20018 Donostia-San Sebastián, Spain.
IKERBASQUE, Basque Foundation for Science, Bilbao, Spain.
E-mail: alejandrojesus.muller@ehu.es

Keywords: triblock terpolymers, triple crystalline spherulites, polymer crystallization.

The morphology, crystallization behavior and properties of multi-crystalline polymer systems based on triple crystalline biodegradable PEO-*b*-PCL-*b*-PLLA triblock terpolymers are reviewed. The triblock terpolymers, with increasing PLLA content, exhibited a triple crystalline nature. Upon cooling from melt, the PLLA block crystallizes first and templates the spherulitic morphology of the terpolymer. Then, the PCL block crystalizes and, lastly, the PEO block. These triblock terpolymers are probably melt miscible, as SAXS experiments confirmed. Thus,

the crystallization of PCL and PEO blocks takes place within the interlamellar zones of the PLLA spherulites that were formed previously. Therefore, the lamellae of PLLA, PCL and PEO exist side-by-side within a unique spherulite, constituting a novel triple crystalline superstructure. The theoretical analysis of SAXS curves implies that only one lamella of either PCL or PEO can occupy the interlamellar space in between two contiguous lamellae of PLLA. Several complex competitive effects such as plasticizing, nucleation, anti-plasticizing and confinement take place during the isothermal crystallization of each block in the terpolymers. New results on how Successive Self-nucleation and Annealing (SSA) thermal treatment can be used as an additional suitable technique to properly separate the three crystalline phases in these triple crystalline triblock terpolymers are also included in this contribution.

1. Introduction

Block copolymers have been in the focus of polymer physics researchers during the past two decades.[1-4] Crystallization and morphology of block copolymers are strictly related with their physical properties and potential applications in several fields. To name a few, block copolymers have been used in biomedical applications, cell adhesion coatings, drug delivery, nanotechnology, stimuli-responsive nanostructured materials, nanoparticles, lithography, patterning and templating in optoelectronics devices, and hydrogels.[5-8] Therefore, understanding the morphology and overall crystallinity is essential for both basic and applied polymer science.[1, 5, 9-12]The final structure, crystallization and physical properties are not only determined by the crystallization conditions but also by the microstructure, chemical nature, molecular weight, block composition and miscibility or segregation between blocks.. [5, 10-22]

Since block copolymers consist of segments of different length and nature, chemically bonded together, a broad range of semicrystalline/amorphous ordered superstructures can be formed, as the polymer chains self-assemble. The superstructures created will depend on the miscibility (or segregation) of the blocks and the transition temperatures (order-disorder, glass

transition and crystallization).[4] Thus, the immiscibility between the blocks or the crystallization process drive the microphase separation that ultimately fixes the final morphology. Nanostructures of different geometries are exhibited by strongly segregated systems, while birefringenced unique mixed spherulites are formed by miscible block copolymers. Those spherulitic-type superstructures include spherulites with well-defined Maltese cross, banded spherulites, concentric spherulites, axialities and 2D aggregates.[5, 12]

Different crystallization phenomena that include nucleating effects, fractionated and confined crystallization, reduced crystallinity, plasticization and retarded or first order crystallization kinetics, have been extensively investigated in miscible diblock and triblock copolymers and terpolymers with more than one crystallizable block.[5, 11, 16-19, 22-24] Particularly, biodegradable and biocompatible diblock copolymers such as poly(ethylene oxide)-*b*-poly(ε-caprolactone) (PEO-*b*-PCL),[25-43] poly(ethylene oxide)-*b*-poly(L-lactide) (PEO-*b*-PLLA),[44-57] and poly(ε-caprolactone)-*b*-poly(lactide)s (PCL-*b*-PLA) [58-68] exhibit two main behaviors: a plasticizing effect over the PLLA crystallization caused by the PCL or PEO molten chains, and both nucleating effect or retarded crystallization kinetics of the crystallization of the PCL and PEO blocks induced by the PLLA previously formed crystals.[6, 17] PLLA-*b*-PCL and PLLA-*b*-PEO diblock copolymers attract high interest, because of their physical properties, as well as, their mechanical performance and biodegradation behaviour, which are in direct relationship with the nano and micro crystalline morphology.[5, 17, 18]

When a third potentially crystallizable block is added, the crystallization behavior and morphology become even more complex. Some authors reported PLLA-*b*-PCL-*b*-PEO-*b*-PCL-*b*-PLLA pentablock terpolymers, in which, according to WAXS experiments, only the PCL and PLLA blocks could crystallize, depending on block composition. For instance, the PCL block crystallized and the PLLA and PEO blocks remained amorphous when the PCL contents increases. On the contrary, if the terpolymer had a higher PLLA content, the PCL melting peak decreased.[69] Thus, very few works have been published for ABC type triblock terpolymers in

which the three blocks have crystalized, particularly, terpolymers with PEO, PCL and PLLA blocks.[34, 70-75] Sun et al. [72] reported triple crystalline triblock and pentablock terpolymers of PLLA, PCL and PEO. They demonstrated the coexistence of the three crystalline structures employing DSC and WAXS analysis. The WAXS spectra exhibited strong diffraction peaks corresponding to the PEO and PLLA crystals but very weak peaks suggesting the presence of PCL crystals. It seems that the PLLA and PEO end blocks highly hamper the crystallization of the PCL middle block. In addition, the PCL content in the terpolymers (between ~13-20 %), is very low, which might be also a reason for the weak WAXS scattering reflections. Complementary DSC analysis was not able to elucidate the crystallization of each block since the crystallization temperature of the PCL and PEO blocks overlapped. However, because PLLA crystalizes at higher temperatures, the crystallization of this block was indeed distinctive. Similar behavior was observed during subsequent melting, since PCL and PEO crystals melt in the same range of temperatures, while the PLLA crystals melted at higher temperatures.

Both block composition and block length are strictly related. Thus, not only the composition influences the crystallizability of the terpolymers. Each block must have a suitable length in order to crystallize. For instance, it is a well known fact that the crystallizability of the PLLA depends on the molecular weight and it exhibits a rather slow crystallization kinetics.[76] In PEO-*b*-PCL-*b*-PLLA triblock terpolymers, Chiang et al.[70] reported that a PLLA block with a molecular weight of 1000 $g.mol^{-1}$ could not crystallizeafter cooling at 10 $^{o}C.min^{-1}$. The molecular weight should had increased up to 6300 $g.mol^{-1}$ in order to obtain a PLLA crystalline phase. But if the PLLA molecular weight is further increased, the crystallizability of PLLA reduces due to its low chain mobility .[76] The authors also reported single crystals obtained from solution. Different crystalline phases were obtained depending on the crystallization protocol employed. In one-step crystallization, not well-defined edge-on PEO crystals were observed while PCL and PLLA crystals were flat-on oriented. On the contrary, in a two-step or a three-step sequential crystallization protocol, the first crystallization of the PLLA block fixed

the final morphology and directed very well-defined single crystals of the PEO and PCL blocks. The PEO and PCL crystallization arose in between the lamellae of the PLLA crystals.

A comprehensive knowledge of this new generation of ABC triblock terpolymers composed of PEO, PCL and PLLA (PEO-*b*-PCL-*b*-PLLA) and their triple crystalline features is highly pertinent. The coexistence in a single superstructure of one amorphous mixed phase including chains of the three blocks, and three unique crystalline phases (each of them corresponding to each block) will affect their physical properties and biodegradability. Herein, we review the latest findings of our group regarding the features of these unique triblock terpolymers. The remarkable tricrystalline structure and the complex crystallization behavior have been studied by wide angle X-ray scattering (WAXS), small angle X-ray scattering (SAXS), differential scanning calorimetry (DSC), atomic force microscopy (AFM), and polarized light optical microscopy (PLOM). New results are also presented after conducting *Successive Self-nucleation and Annealing* (SSA) thermal protocols [77, 78] in this kind of terpolymers.

2. The ABC triple crystalline triblock terpolymers under study

The triblock terpolymers under study were synthesized previously, as reported in ref. 79. The structure of the PEO-*b*-PCL-*b*-PLLA triblock terpolymers are presented in **Figure 1**.

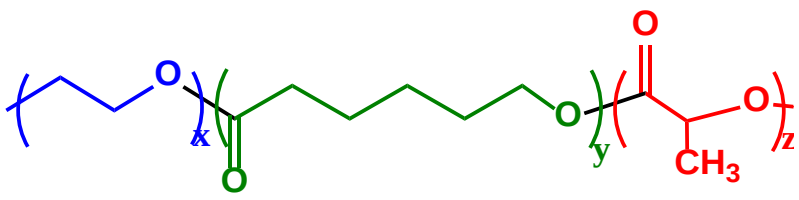

PEO-*b*-PCL-*b*-PLLA triblock terpolymer

Figure 1. Chemical structure of the PEO-*b*-PCL-*b*-PLLA triblock terpolymers

One-pot sequential organocatalytic ring-opening polymerization of ethylene oxide (EO), ε-caprolactone (CL) and L-lactide (LLA) using benzyl alcohol as the initiator and a phosphazene base, 1-*tert*-butyl-2,2,4,4,4-pentakis(dimethylamino)-2λ^5,4λ^5-catenadi(phosphazene) (*t*-BuP_2), as a single catalyst for the three monomers, was employed. Extensive details of the synthesis of the terpolymers can be found in reference.[79, 80] The triblock terpolymers have the same lengths of PEO and PCL blocks and different lengths of PLLA blocks (see Table 1). The corresponding PCL-*b*-PLLA diblock copolymers and PEO, PCL and PLLA homopolymers were synthesized similarly and were included only for comparison purposes. The synthesis methodology allowed guaranteeing relatively narrow molecular weight distributions (ĐM < 1.20). The chemical structure was confirmed by nuclear magnetic resonance spectra (^{1}H NMR). Size exclusion chromatography (SEC) and ^{1}H NMR were used to stablish the number-average molecular weight (M_n) of the blocks and the M_n of the entire terpolymers and corresponding diblock copolymers.

All the samples are described in Table 1, being thethe subscript numbers the composition of theblocksand the superscript numbers, the molecular weight of the entire terpolymer, diblock copolymer or homopolymer.

Table 1. Block molecular weight (M_n) and polydispersity index (PDI) of the terpolymers, diblock copolymers and homopolymers.

Sample code	M_n PEO block (g mol^{-1})	M_n PCL block (g mol^{-1})	M_n PLLA block (g mol^{-1})	PDI (Mw/Mn)
PEO^{4}	3800	-	-	1.03
PCL^{7}	-	7000	-	1.10
$PLLA^{4.6}$	-	-	4600	1.10
$PLLA^{8.6}$	-	-	8600	1.12
$PCL_{59}PLLA_{41}^{11.2}$	-	6600	4600	1.21
$PEO_{29}PCL_{42}PLLA_{29}^{16.1}$	4600	6800	4700	1.10
$PCL_{43}PLLA_{57}^{15.4}$	-	6600	8800	1.16
$PEO_{23}PCL_{34}PLLA_{43}^{19.9}$	4600	6800	8500	1.18

3. Standard SAXS characterization of the PEO-*b*-PCL-*b*-PLLA triblock terpolymers

SAXS experiments in the melt demonstrated that both triblock terpolymers investigated (see Table 1) are probably melt miscible. No reflection was observed at 160 ºC, a temperature at which both samples are in molten state. The lack of SAXS scattering is an indication of a homogeneous phase. However, it should also be considered that the electron density difference between the phases (i.e., PLLA, PCL and PEO) could be too small for weak segregation to be detected. [29] Nevertheless, as PLLA can form spherulites or axialites during crystallization from the melt, such crystallization must be taken place from a melt mixed or weakly segregated melt

Despite that, a homogeneous melt (or only weak segregation) is a common observation in PCL-*b*-PEO[17], PCL-*b*-PLLA,[60, 65, 66] and PEO-*b*-PLLA[48] diblock copolymers. The melt microphase segregation in diblock copolymers can be predicted by calculating the segregation strength (which is the product of the Flory-Huggins interaction parameter (χ) and the polymerization degree (N), on the basis of the mean-field theory[3, 20]). Since the samples are ABC-type triblock terpolymers, it is more complicate to estimate their miscibility through this theory. A rough estimation of χ [49, 68, 81] and χN parameter for each pair of blocks AB, BC and AC of PEO, PCL and PLLA in the terpolymer (the solubility parameters used are reported in the literature[49, 68]) indicates a low melt-segregation, since the χN values of the pairs are lower than 10. Even though the χN values do not fully represent the interactions in the triblock terpolymer as a whole, they did agree well with what it was expected. Both the literature reports about similar diblock copolymers and the SAXS experiments of both PEO-*b*-PCL-*b*-PLLA triblock terpolymers agreed and confirmed the block miscibility in the melt.

As the terpolymers are cooled down from melt, SAXS scattering peaks are observed at room temperature and 80 ºC. These peaks imply the presence of a long-range order periodic

lamellar microdomain structure.[82] For instance, PEO-*b*-PCL diblock copolymers exhibited analternating crystalline lamellar structure, in which an amorphous layer is in between a lamella of PCL and a lamella of PEO.[82] Similar alternating lamellar structures has also been reported on diblock copolymers of PLLA with either PCL or PEO(PEG) (see [5, 17] and references therein), which are all weakly segregated or miscible in the melt. The nature of the lamellar structure and morphology in these triblock terpolymers will be the subject of the upcoming sections, but first, the crystallizability of each block is assessed by DSC and WAXS analysis.

4. Non-Isothermal crystallization of PEO-*b*-PCL-*b*-PLLA triblock terpolymers evaluated by DSC and WAXS analysis

The thermal behaviour of the samples affects their final morphology. The DSC and WAXS experiments demonstrate that these ABC triblock terpolymers are triple crystalline upon cooling from the melt (see **Figure 2**). The triple crystalline nature is achieved when slow cooling rates are used (between 1 and 5°C.min^{-1}). The DSC cooling scan of the terpolymers exhibits three well-defined exothermic peaks that correspond to the crystallization of each block from the melt (see **Figure 2b**). The PLLA block crystallizes first at expected temperature, around 70 ºC. Upon further cooling after PLLA crystallization, the PCL or the PEO block could crystallize but which one did it first is very difficult elucidate, since both blocks have similar crystallization temperatures. Analogous PEO-*b*-PCL-*b*-PLLA triblock terpolymers obtained by Chiang et al by a different synthetic pathway exhibited a similar behavior.[83]

The order of crystallization depends on copolymer composition. For instance, in PEO-*b*-PCL diblock copolymers, the PCL block crystallizes first than the PEO block when PCL is the major component. On the contrary, the PEO block crystallizes first, when its content in the copolymer is higher. WAXS measurements, taken upon cooling from melt, allowed us to identify the order in which each block crystallized from the melt. The crystallographic planes of PEO, PCL and PLLA crystalline structures were determined, and the crystallization order

goes as follows: the PLLA block crystallizes first, then the PCL block, and at the end, the PEO block. In this case, the crystallization sequence observed in the triblock terpolymers obeyed to the larger PCL content.

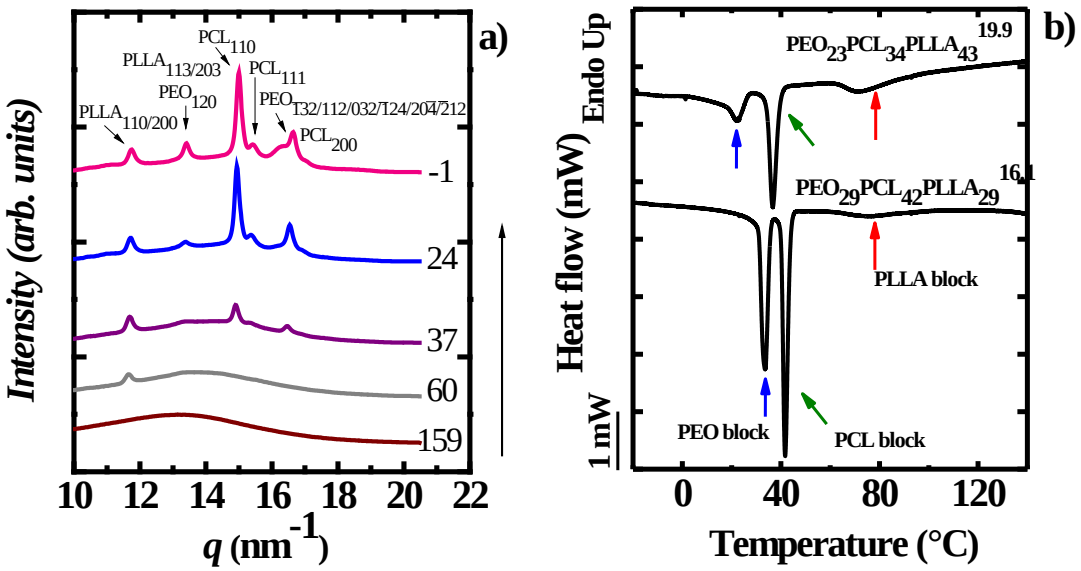

Figure 2. (a) WAXS pattern taken at different temperatures during cooling from the melt at 5 ºC min^{-1} of $PEO_{29}PCL_{42}PLLA_{29}^{16.1}$. (b) DSC cooling scans at 1 ºC min^{-1} after melting at 160 ºC for 3 min. Reproduced with permission.[71] Copyright 2016, RSC.

5. Microscale morphology of the PEO-*b*-PCL-*b*-PLLA triblock terpolymers

Several aspects influence the solid-state arrangement of block copolymers: crystallization behavior, block copolymer composition, segregation strength and microphase separation due to the crystallization process. The sequential crystallization and superstructural organization of the terpolymers can be detected by Polarized light optical microscopy (PLOM) microscopy in samples cooled from the melt.

Since these triblock terpolymers are melt-miscible, the block that crystallizes first upon cooling from the melt (i.e. the PLLA block) fixes the microscale morphology of the whole terpolymer. [71] The phase separation is driven by the PLLA block crystallization, which in the end templates the morphology for the following crystallization of the PCL and PEO blocks.

Irregular spherulitic-type superstructures[71] without banding extinction patterns is the microscale morphology of the terpolymers observed by PLOM (see **Figure 3a,a'**).

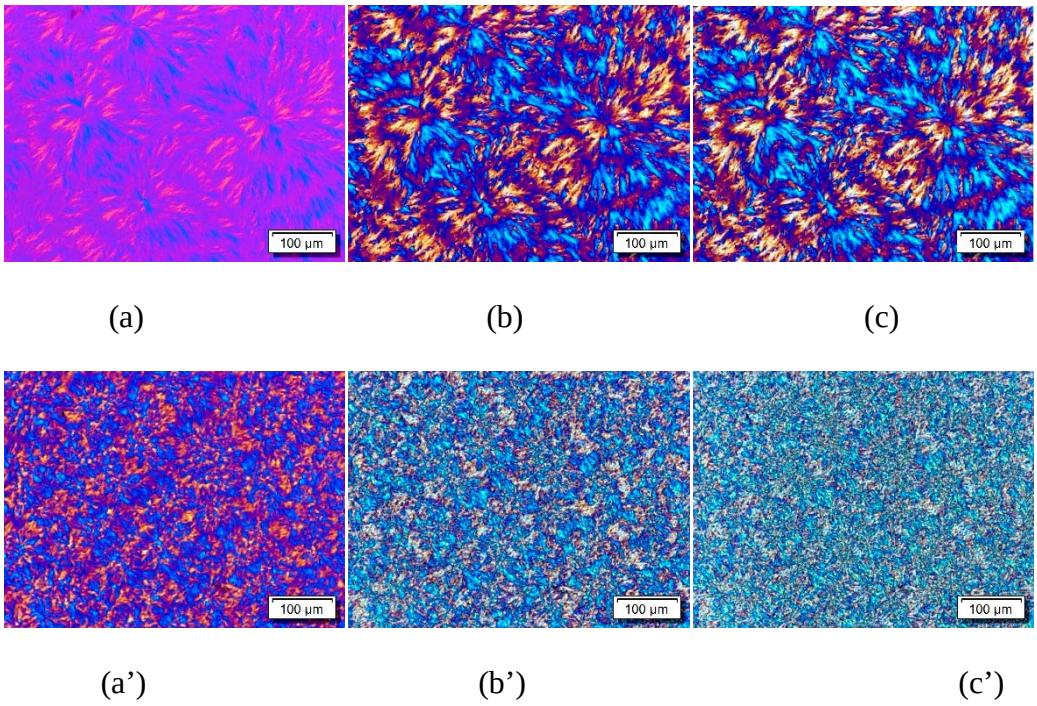

Figure 3. PLOM Micrographs taken at a) a') 100 ºC, b) b') 39 ºC and c) c') room temperature for $PEO_{29}PCL_{42}PLLA_{29}^{16.1}$ (up) and $PEO_{23}PCL_{34}PLLA_{43}^{19.9}$ (down). Scale bar 100 µm. Reproduced with permission.[73] Copyright 2018, Elsevier Inc.

As the PLLA content in the terpolymer is reduced, a branch-like morphology is developed by this block. This irregular crystalline texture might be due to a disturbance of the PLLA lamellae growth caused by a richer PCL-PEO amorphous phase in the proximity of the crystalline front.[49] After PLLA crystallization, the sample is further cooled down and a change in the magnitude of the birefringence takes place, without altering of the PLLA superstructure. This birefringence change is caused by the PCL crystallization that is taking place within the interlamellar regions of the PLLA spherulites that were formed before. (see **Figure 3b,b'**). Similar as in miscible PCL-*b*-PLLA[63-66] and PEO-*b*-PLLA[51, 55, 56] diblock copolymers reported previously.

Further cooling after PCL crystallization only caused a new change in the magnitude of the birefringence: the quadrant colors became even lighter and brighter. This additional change in the magnitude of birefringence is due to the crystallization of the PEO block. In other words, the subsequent crystallization of the PCL block, second, and the PEO block, third, did not modify significantly the superstructure created during PLLA crystallization, and only a sequential change in the magnitude of the birefringence occurred due to the intraspherulitic crystallization of the PCL and PEO blocks within the PLLA interlamellar regions (see **Figure 3c,c'**).

These PLOM observations in the $PEO_{29}PCL_{42}PLLA_{29}^{16.1}$ and $PEO_{23}PCL_{34}PLLA_{43}^{19.9}$ triblock terpolymers are very similar to those reported on PCL-*b*-PLLA [17, 64-66] and PEO-*b*-PLLA [51, 55, 56] diblock copolymers. The final microscale morphology is a mixed spherulitic-type superstructure with crystalline lamellae of PLLA, PCL and PEO surrounded by an amorphous phase that includes PLLA, PCL and PEO chains.[71]

6. Nanoscale morphology of the PEO-*b*-PCL-*b*-PLLA triblock terpolymers

The way the three types of lamellae arrange inside the spherulitic morphology was assessed by detailed SAXS/WAXS analysis and AFM observations, after employing different crystallization protocols.[74] Since these are melt-miscible triblock terpolymers, it might be assumed that the mixed spherulitic-type superstructures are composed of lamellae from each constituent block interdigitated and alternated between them. In order to give evidences of this hypothetic alternated lamellar crystalline structure at the nanoscale, a thermal protocol was employed and the final lamellar morphology of the samples was observed by AFM.

The terpolymers were first crystallized at the PLLA crystallization temperature until saturation, then quenched until PCL crystallization temperature and allowed crystallizing until saturation, and finally, quenched until room temperature. During this last cooling, the PEO block also crystallizes. An outstanding picture of the tricrystalline structure of the PEO-*b*-PCL-

b-PLLA triblock terpolymers is depicted in the images obtained by AFM microscopy (see **Figure 4**).

The triblock terpolymers exhibited a wide range of lamellae of different thicknesses (**Figure 4**). Three average populations of different lamellar thickness were detected and measured. The thicker edge-on lamellae have 15 nm (an example is labeled red in **Figure 4**), and the second average lamellar thickness observed is around 10 nm (examples are labeled green in **Figure 4**). Comparisons made with an analogous PLLA-*b*-PCL diblock copolymer (precursors) of the same molecular weight subjected to the same thermal protocol allows assigning the thickest lamellae to the PLLA block and the 10 nm lamellae to the PCL block.

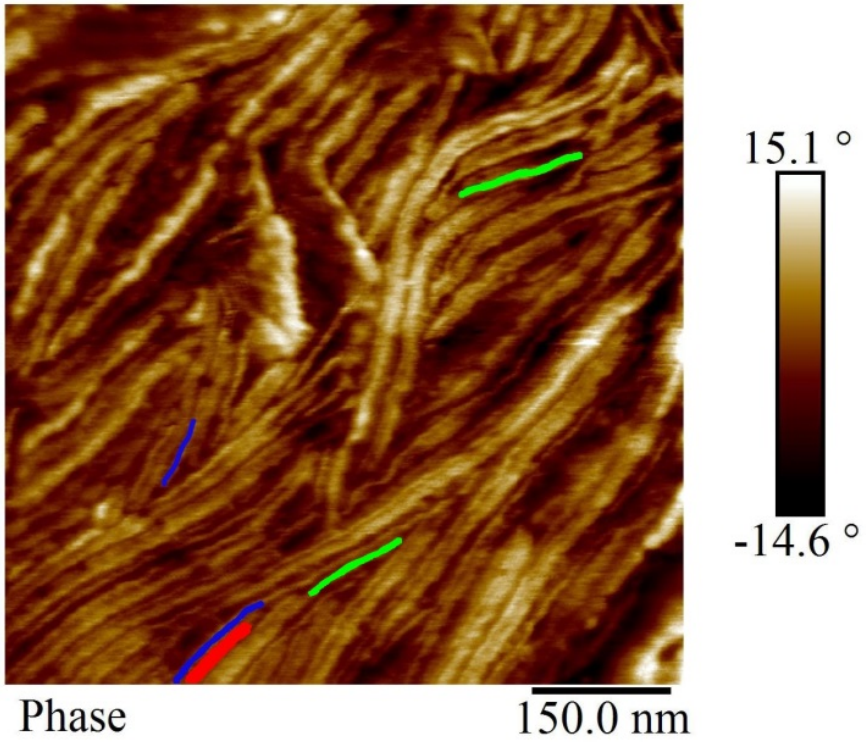

Figure 4. AFM phase micrographs of $PEO_{23}PCL_{34}PLLA_{43}^{19.9}$ observed at 25 ºC, where three different average lamellar thickness are observed corresponding to the three constituent blocks (see text). Samples were quenched to 25 ºC after isothermal crystallization in two steps: first at 81 ºC and then at 50 ºC. Reproduced with permission.[74] Copyright 2017, ACS.

Besides the 15 nm and 10 nm lamellae, an additional and even smaller average lamellar thickness was observed in the terpolymer by AFM. This third population of lamellae was measured and exhibited an average lamellar thickness of ~ 7 nm (examples are labelled blue in

Figure 4). These lamellae should correspond to the PEO block. In order to prove that the three crystalline phases (PEO, PCL and PLLA) were present in the terpolymer, a WAXS pattern was taken at 25 ºC. The crystallographic planes of the three PLLA, PCL and PEO crystals were observed in the WAXS spectrum. However, the PEO_{120} reflection overlaps with the $PLLA_{113/203}$ peak. Thus, it is difficult to infer with certainty that the PEO block also crystallized. To resolve this, SAXS/WAXS patterns were taken upon heating the crystallized terpolymer and the corresponding diblock copolymer samples.

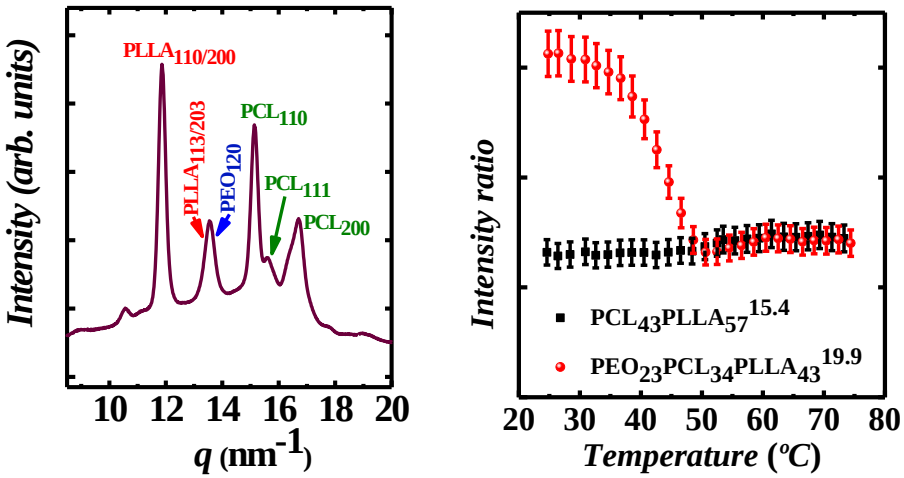

Figure 5. a) WAXS patterns of $PEO_{23}PCL_{34}PLLA_{43}^{19.9}$ taken at 25 ºC, after isothermally crystallizing the sample in two steps: first at 81 ºC and then at 49.5 ºC. b) Intensity ratio between WAXS signals $PLLA_{113/203}$ and $PLLA_{110/200}$ of $PCL_{43}PLLA_{57}^{15.4}$, and ($PLLA_{113/203}$+PEO_{120}) and $PLLA_{110/200}$ of $PEO_{23}PCL_{34}PLLA_{43}^{19.9}$ during heating after crystallizing the samples in two steps. Reproduced with permission.[74] Copyright 2017, ACS.

The intensity ratio between $PLLA_{113/203}$+PEO_{120} and $PLLA_{110/200}$ reflections of the $PEO_{23}PCL_{34}PLLA_{43}^{19.9}$ terpolymer was measured and compared to the $PLLA_{113/203}$ and $PLLA_{110/200}$ WAXS reflections of the corresponding $PCL_{43}PLLA_{57}^{15.4}$ diblock copolymer (see **Figure 5a**). If the PEO block in the terpolymer also crystallized, the intensity of its crystalline reflection (at the PEO_{120} signal) would be included into the intensity measured for the $PLLA_{113/203}$ reflection.

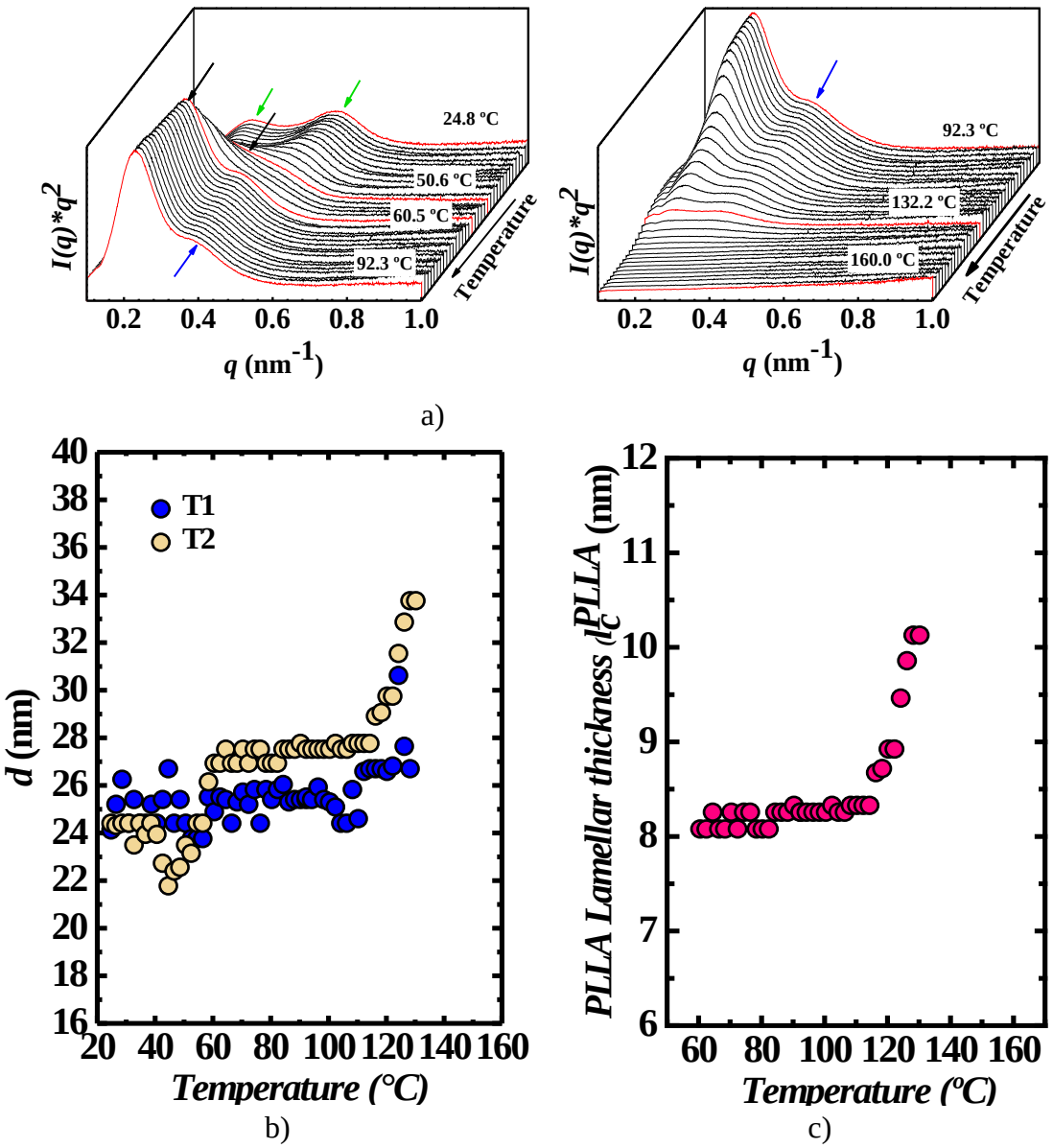

Figure 6. a) Lorentz corrected SAXS patterns during heating of $PEO_{23}PCL_{34}PLLA_{43}^{19.9}$, after isothermally crystallizing the sample in two steps: first at 81 ºC and then at 50 ºC. b) Evolution of the long period values calculated from SAXS measurements during heating, after isothermally crystallizing $PEO_{23}PCL_{34}PLLA_{43}^{19.9}$ at 81 ºC (T1), and at 81ºC and then 50 ºC (T2). c) Evolution of the PLLA lamellar thickness during heating, after isothermally crystallizing the sample in two steps: first at 81 ºC and then at 50 ºC. Reproduced with permission.[74] Copyright 2017, ACS.

Between 25 and 75 ºC, the intensity ratio of the diblock copolymer does not vary significantly (see black symbols). In this temperature range the PLLA phase remained crystalline (see **Figure 5b**). On the contrary, at 25 ºC, the terpolymer exhibited an intensity ratio

that was almost twice the value of the one shown by the corresponding the diblock copolymer (see **Figure 5b**). Thus, the presence of a PEO crystalline phase in the $PEO_{23}PCL_{34}PLLA_{43}^{19.9}$ triblock terpolymer is confirmed by this experiment. Further increment of the temperature up to 50 °C reduced the intensity ratio in the terpolymer until it matches the intensity ratio of the diblock copolymer. DSC measurements demonstrated that the PEO block melts at 45 ºC. As conclusion, the WAXS experiments demonstrated without doubt the exceptional tricrystalline structure observed by AFM for this ABC type triblock terpolymer.[74]

The nanoscale structure was assessed employing also X-Ray experiments. SAXS/WAXS measurements were taken of the as crystallized triblock terpolymer at room temperature, and then during a subsequent heating (see **Figure 6a**). The evolution of the long period (*d*) value was registered as a function of temperature.[74] It is very difficult to certainly assign the SAXS peaks to a particular population of lamellae in the triblock terpolymer, since the alternated lamellar structure in which the three blocks co-exist is not that clear. The long periods measured are an average value of the crystalline lamellar phases present. Hypothetically, the PLLA lamellae that crystallized first should be responsible for the scattering of the larger domain spacing.

Figure 6a shows that two transitions occurred at around 50 and 60 ºC. Between these temperatures a significant increment in the intensity of the first SAXS peak can be seen and a modest increment in the long period values (*d*). The first transition coincides with the melting of the PEO block, and the second one with the melting of PCL block. Beyond 60 ºC, the PLLA block is the only one that remained crystalline and its interlamellar regions are composed of mixed amorphous phase that include PLLA, PCL and PEO chains. Finally, at around 120 ºC, the long period values and, accordingly, the PLLA crystalline lamellar thickness increased (see **Figure 6b** and **c**).[74]

The SAXS analysis of the PLLA block become more complex to elucidate due to the crystal reorganization phenomenon that is characteristic of PLLA during heating. After the melting of

PCL and PEO blocks, a high-*q* shoulder can be observed in Figure 6a (signaled with a blue arrow). The analysis demonstrated that this small shoulder should correspond to a second order reflection, and not to a second population of PLLA crystals of smaller lamellar thickness. If it was so, these smaller PLLA crystals should have melted at lower temperatures and the shoulder should have disappeared at those temperatures, but that is not the case. Both peak and shoulder disappeared almost simultaneously beyond 132 °C.[74]

After the PEO and PCL blocks melting (at around 65 ºC), the lamellar thickness of the PLLA crystals in the triblock terpolymer was ~8.3 nm (see **Figure 6c**), which is similar to the value reported by Xue et al.[29] in symmetric PLLA-*b*-PEO diblock copolymers.[74] Considering this value, a three-fold chain conformation was estimated and proposed for the PLLA block. Similarly and taking into account the lamellar thickness measured by both AFM and SAXS and the length of the extended chain, the PCL and PEO blocks should have also crystallized in a multi-folded arrangement.

7. Elucidating the tri-lamellar packaging of the PEO-*b*-PCL-*b*-PLLA triblock terpolymers

The way the coexisting three types of lamellae arrange inside the triple crystalline terpolymer spherulites is intriguing. After the crystallization of the PLLA block, the crystallization of the PCL and PEO blocks takes place inside the mixed interlamellar amorphous regions of the PLLA spherulites. Thus, it is very complex to resolve the lamellar self-assembly within the triblock terpolymers, since the mixed amorphous domains contain both PCL and PEO chains. It is complicate to ascertain the exact tri-lamellar packing inside the spherulite, once these other two blocks have crystallized.. With the purpose of elucidating this question, one-dimensional structural models have been employed.[74]

The experimental SAXS curves were theoretically reproduced employing one-dimensional density profiles $\rho(x)$ from microstructural models (see **Figure 7a**). Several suppositions were

considered. First, the whole system was described as a one-dimensional problem (ignoring the contribution microphase separation because these triblock terpolymers exhibited miscibility in the melt). Second, a Gaussian distribution of the long period of PLLA, and theoretical values for long period and standard deviation were assumed. Thus, the intensity $I(q)$ can be calculated numerically from the absolute square of the Fourier transform of the scattering density, according to scattering theory. In this way, the periodic lamellar structure can be theoretically described.

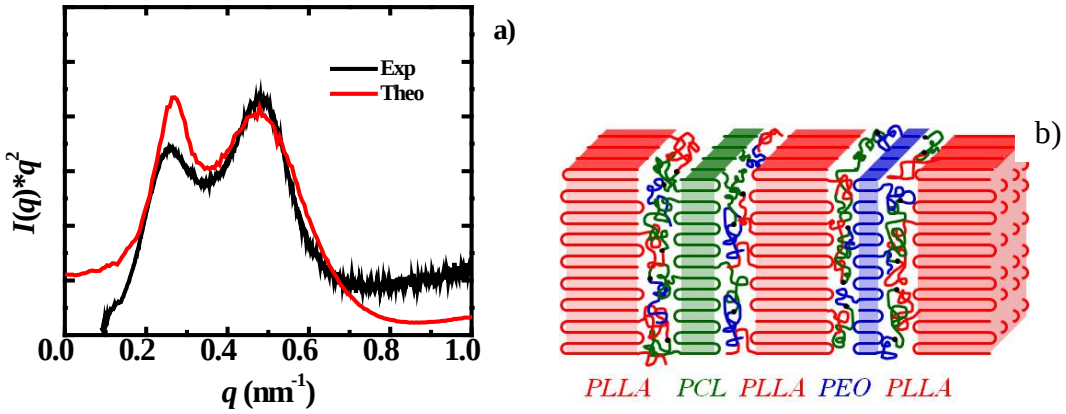

Figure 7. a) Experimental SAXS data at 25.3 ºC and simulated SAXS curve of the density profile corresponding to crystalline PCL and PEO. b) Schematic representation of the trilayered morphology in the triple crystalline $PEO_{23}PCL_{34}PLLA_{43}^{19.9}$ triblock terpolymer. Reproduced with permission.[74] Copyright 2017, ACS.

After several trails, the array model that best fitted the experimental data was an insertion model in random fashion (**Figure 7b**), in which only a PCL or a PEO crystalline lamella is inserted within the PLLA amorphous layer, that is in the intelamellar region in between PLLA lamellae. The purpose of the simulation is to have a qualitative picture of the microstructure by comparing experimental scattering SAXS curves with the theoretical ones, instead of obtaining the exact structural parameters. Thus, the trilamellar morphology proposed include only one lamella of PCL or one lamella PEO that inserts randomly between two lamellae of PLLA [74] (see **Figure 7b**).

8. Overall isothermal crystallization kinetics of the PEO-*b*-PCL-*b*-PLLA triblock terpolymers

Different crystallization phenomena have been reported in double crystalline diblock and triblock copolymers. Adding a third crystallizable block complicates even more the understanding of the crystallization behaviour of these multiphasic materials, since each block and the environment created affects the crystallization of the other two. Therefore, different sequential crystallization protocols were designed and implemented to follow the isothermal crystallization behavior of each block in the PEO-*b*-PCL-*b*-PLLA triblock terpolymers,

8.1 Isothermal crystallization kinetics of the PLLA block

The isothermal cold crystallization of the PLLA block (i.e., crystallizing from the glassy state) in the triblock terpolymers was followed after quenching from melt state until 0°C and subsequent heating until the PLLA crystallization temperature was reached. This methodology was chosen in order to increase the nucleation density of the very slow-crystallizing PLLA block. Comparisons were made with analogous PLLA-*b*-PCL diblock copolymers of same molecular weight of the blocks in order to establish differences.

The PCL and PEO blocks are molten during the crystallization of the PLLA block, since this block crystallizes at higher temperatures. Thus, the molten PCL and PEO chains plasticized the PLLA block, causing an increment in the supercooling needed to crystallize de PLLA block (see **Figure 8, left**). Despite the plasticizing effect, an unexpected improvement on the overall crystallization rate of the PLLA block in the terpolymers was observed, in comparison to the crystallization rate of the same PLLA block in the analogous diblock copolymer. This behavior contradicts the PLLA block crystallization reports in PCL-*b*-PLLA diblock copolymers, in which it has been observed a diminishment of the crystallization rate of the PLLA block.[63]

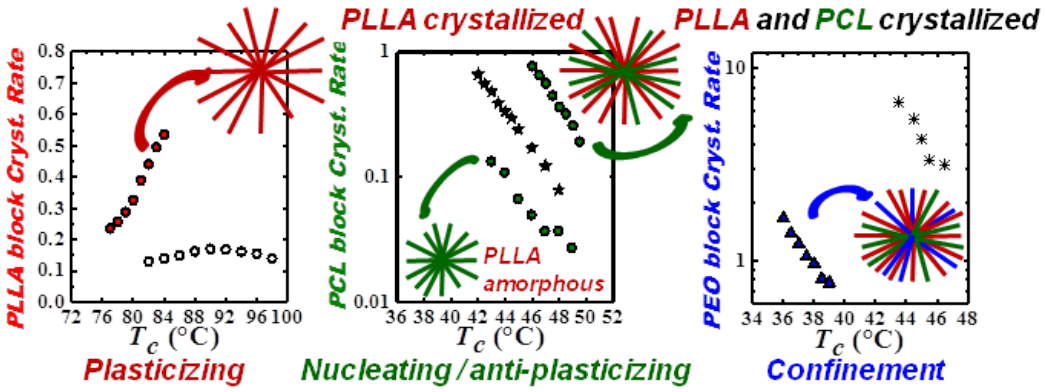

Figure 8. Schematic representation of overall isothermal crystallization behaviour of PLLA (red, left), PCL (green, center) and PEO (blue, right) blocks in PEO-*b*-PCL-*b*-PLLA triblock terpolymers. Reproduced with permission.[75] Copyright 2017, ACS.

The enhanced crystallization of the PLLA block in the terpolymers might be related to the high mobility of the additional and extremely flexible PEO chains that might contribute to the diffusion of the PLLA chains into the growing crystalline front. This plasticizing effect of the molten PEO and PCL chains might increase the supercooling needed in order to induce the crystallization of the PLLA block (please be aware that PLLA isothermal crystallization was followed upon heating from 0 ºC, i.e., cold isothermal crystallization).

A particular observation is that the increment in the PLLA block molecular weight caused a slightly reduction of the PLLA crystallization rate at the same temperature. That is a common observation for PLLA.[76, 84] In addition, the crystallization degree of the PLLA block is smaller in both terpolymers than in the diblock copolymers. The lower crystallinity degree is an indication of the plasticizing effect induced by the molten PCL and PEO chains, which content is higher in the terpolymers. In other words, it might become more difficult to add new crystallizable segments to the crystallization front due to the diluent effect induced by the molten PEO and PCL chains. Finally, the experimental data was fitted to the Avrami equation. The Avrami index values obtained agreed with instantaneously nucleated axialites (or 2D aggregates) in the terpolymers and with instantaneously nucleated spherulites in case of the diblock copolymers.[75]

8.2 Isothermal crystallization kinetics of the PCL block

The crystallization behavior of the PCL block in the terpolymers and diblock copolymers was followed under two different crystallization protocols. Comparisons were made with a PCL homopolymer of the same molecular weight as in the terpolymers and diblock copolymers. In the first protocol (protocol 1) (see **Figure 9**, left), the PLLA block was first crystallized until saturation, and then, the sample was quenched until the crystallization temperature of the PCL block and the isothermal PCL crystallization was recorded. The purpose of this thermal protocol was to evaluate the influence of the PLLA semicrystalline matrix surrounding the PCL chains in the PCL block crystallization.

In a second protocol (protocol 2) (see **Figure 9, right**), the sample was quenched directly from the melt until the crystallization temperature of the PCL block, in order to follow the isothermal PCL block crystallization surrounded by a PLLA phase in amorphous state... In both protocols, the PCL block was crystallized at temperatures in which the third PEO block stayed molten.[75]

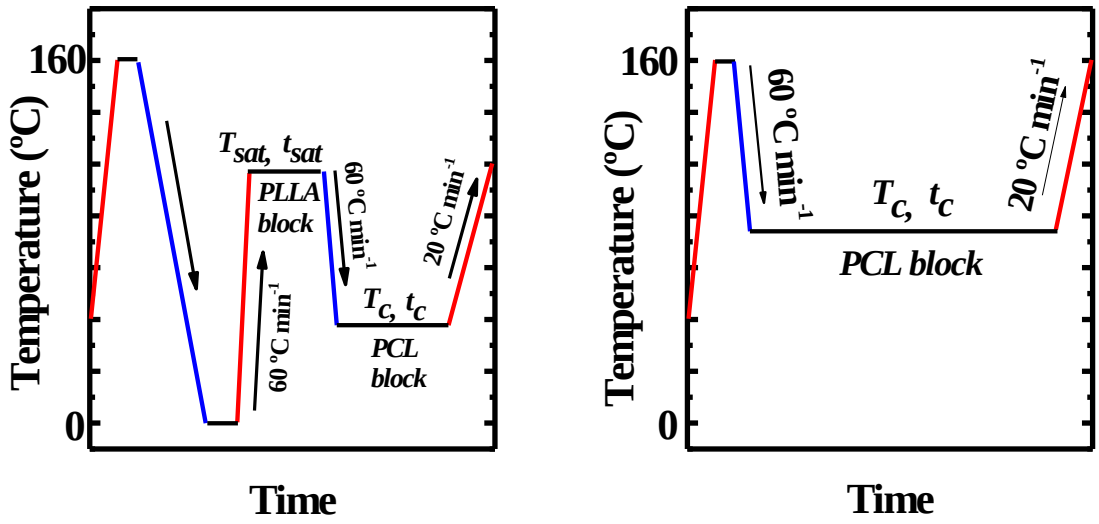

Figure 9. Two step crystallization protocol (protocol 1) employ to follow the isothermal crystallization of the PCL block with the PLLA phase previously crystallized (left). One step crystallization protocol (protocol 2) to follow the crystallization of the PCL block while keeping the PLLA phase amorphous (right).

8.2.1 Protocol 1: Semicrystalline PLLA matrix

Even though the PCL block had to crystallize inside the interlamellar regions of the previously formed PLLA crystals, the crystallization kinetics of the PCL block was faster in the terpolymers and diblock copolymer than in the PCL homopolymer. Moreover, the supercooling needed to crystallize the PCL block reduced. Those observations are an indication of a nucleating effect caused by the PLLA crystals over the PCL crystallization (see **Figure 8, center**, PLLA matrix crystallized). In addition, richer PCL domains are induced by the previous crystallization of the PLLA block. During the PLLA crystallization, the PCL and PEO chains are excluded from the crystallization front, leading to richer domains of PCL and PEO. Thus, during the crystallization of the PCL block, the subsequent diffusion of the PCL chains to the crystallization front is less hindered, promoting an acceleration in the PCL crystallization kinetics.

Comparing the terpolymer with the diblock copolymer (both with smaller PCL content), it should be noted that the PCL block is in the middle and had one end attached to a molten PEO chain and the other to a PLLA crystal. It seems that the PEO molten block improved the PCL block crystallization. This suggested that the molten PEO chain, chemically bonded to one end of the PCL block, might increase the diffusion and mobility of the PCL chains to the crystallization sites. Therefore, a slight increment in the overall PCL crystallization kinetics was detected. The amorphous PEO molten chains also aided to augment the PCL crystallinity degree, as if we compared to the crystallinity of the PCL block in the diblock copolymers. Increased mobility and diffusion of the PCL chains to the growing PCL crystal front might have contributed to the enhanced PCL crystallinity.[75]

8.2.2 Protocol 2: Amorphous PLLA matrix

The opposite crystallization behavior was observed for the PCL block in the terpolymers under this condition. The crystallization kinetics of the PCL block in the terpolymers and diblock copolymers was highly reduced, as compared to the PCL homopolymer. The surrounding amorphous PLLA phase induced an anti-plasticizing effect that caused a reduction of the overall crystallization kinetics. In addition, the supercooling needed to crystallize the PCL block under this condition enlarged (see **Figure 8, center**, PLLA matrix amorphous). A reason for the observed behavior might be a demixing process suffered by the PCL chains from a mixed amorphous phase that contains more rigid PLLA chains. This demixing process is required in order to nucleate and grow in the crystalline front. The PCL block crystallizes at temperatures in which the chain movements of the more rigid PLLA block are slower, making more difficult the crystallization of the PCL chains covalently attached to them. However, comparing with the diblock copolymer, a third molten PEO block (as in the terpolymers) enhanced the crystallization kinetics of the PCL block in the middle, increased the crystallization temperature, and therefore, reduced supercooling needed to crystallize.

As in protocol 1, the molten PEO chains in the terpolymers caused a plasticizing effect, enhancing the crystallization ability of the PCL block. The molten PEO chains might increase the diffusion and mobility of the PCL chains to the crystalline front. Despite the fact that PEO molten chains improved the crystallization rate, the PCL block crystallinity degree did not significantly change in the diblock copolymer and terpolymer in the supercooling range evaluated. In addition, fitting to the Avrami equation provided Avrami index values between 2 and 3.[75]

8.3 Isothermal crystallization kinetics of the PEO block

Following the isothermal crystallization kinetics of the third PEO block alone is very complex because the PEO crystallization and melting temperatures are very close to those of the PCL block. Thus, a crystallization protocol in three sequential steps was needed in order to

ensure that only the PEO block was crystallizing at the selected crystallization temperatures. . The thermal protocol comprised a first crystallization of the PLLA block until saturation. Then, in a second step, the as crystallized sample was rapidly cooled down to the PCL crystallization temperature and this block was crystallized until saturation. The PCL crystallization temperature was chosen to be high enough in order to keep the PEO chains melted. Finally, in a third step, the sample was again rapidly cooled down until the PEO crystallization temperature and the PEO isothermal crystallization was registered. In this way, it was evaluated the effect of the previously formed PLLA and PCL lamellae on the PEO block crystallization in the terpolymer.

Both PLLA and PCL crystalline lamellae imposed a confinement effect over the PEO crystallization, reducing its crystallization, kinetics in comparison to the PEO homopolymer. Moreover, the PEO block crystallized at lower crystallization temperatures. Thus, a higher supercooling was required to induce the PEO block crystallization (see **Figure 8, right**). The previously formed PCL and PLLA crystals constituted a hard confinement case. In other words, the PCL and PLLA lamellae established a hard environment surrounding the amorphous mixed phase that included the PEO block chains. As it was proposed by the theoretical SAXS analysis, the PEO chains may have only crystallized in the limited free interlamellar spaces between the PLLA lamellae, but only those spaces in which none PCL lamella grew first. The proposed model suggested that the PLLA interlamellar zones are not big enough to hold both PCL and PEO block lamellae together. Therefore, the PCL and PLLA lamellae hindered the PEO block crystallization, reducing both its crystallization rate and its crystallinity degree, in comparison to the PEO homopolymer.

[75]

9. Melting behavior and thermal fractionation of the PEO-*b*-PCL-*b*-PLLA triblock terpolymers by means of Successive Self-nucleation and Annealing (SSA) protocol

The melting behavior of these ABC triblock terpolymers was analized by DSC. In order to obtain a tricrystalline terpolymer (that is a triblock terpolymer in which all the block could crystallize separately), it is of major importance to employ very small crystallization rates (1°C.min^{-1}). Beyond this value, it is not possible to identify in a DSC the crystallization of the PEO and PCL blocks independently, since their inherent crystallization temperatures are very close. The same problem occurs with their melting temperatures.

Figure 10 depicts the DSC heating scan at 20 °C.min^{-1}, after crystallizing the samples at 1°C.min^{-1}, of both PEO-*b*-PCL-*b*-PLLA triblock terpolymers. The melting of the PLLA block clearly takes place at around 120 ºC, identified by a broad endothermic peak with a minor low-temperature shoulder, that is ascribed to a recrystallization-melting mechanism.[63, 85-87] The PEO and PCL crystals melt at lower temperatures between 40 and 60 ºC. A double endothermic peak located between these temperatures indicates the melting of these blocks, but is not possible to separate them by a standard cooling and heating DSC scan.

A highly useful thermal fractionation technique is Successive Self-Nucleation and Annealing (SSA). It was designed and implemented by Müller et al.[77, 78] and it is conceptually based on the molecular segregation capacity exhibited by semicrystalline polymeric systems when they are isothermally crystallized or annealed. As advantages, SSA can thermally fractionate a polymer sample in a short time, employing standard DSC equipment. It consists on the sequential application of self-nucleation and annealing steps to a polymer sample. The final DSC heating run reveals the distribution of melting points induced by the SSA protocol. In order to properly apply the technique, a previous Self-Nucleation (SN) thermal protocol must be conducted in the samples. This protocol allows obtaining the Ideal Self-Nucleation temperature (T_s), which will be the starting temperature of SSA.

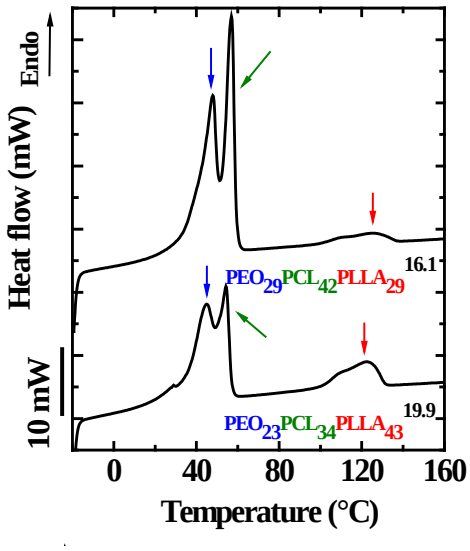

Figure 10. Subsequent DSC heating scans at 20 ºC min^{-1} after cooling at 1 ºC min^{-1} of the PEO-*b*-PCL-*b*-PLLA triblock terpolymers. Reproduced with permission.[71] Copyright 2016, RSC.

Therefore, in order to apply the SSA thermal fractionation treatment to the terpolymers and the corresponding diblock copolymers and PLLA homopolymers, we selected the sample with the highest PLLA melting temperature and conducted a self-nucleation protocol (see **Figure 11a**) on it. The aim is to produce self-nuclei by partial melting of a standard crystalline state (see reference[77, 78] for more details). From the SN experiments, the Domains of Self-Nucleation can be determined. Depending on the T_s chosen, the polymer can melt entirely, only self-nucleate or self-nucleate and anneal. The ideal T_s temperature is the lowest temperature within the self-nucleation domain. It can be identified as that temperature prior to that one that produces a characteristic annealing peak (i.e., domain III) in the subsequent melting scan.

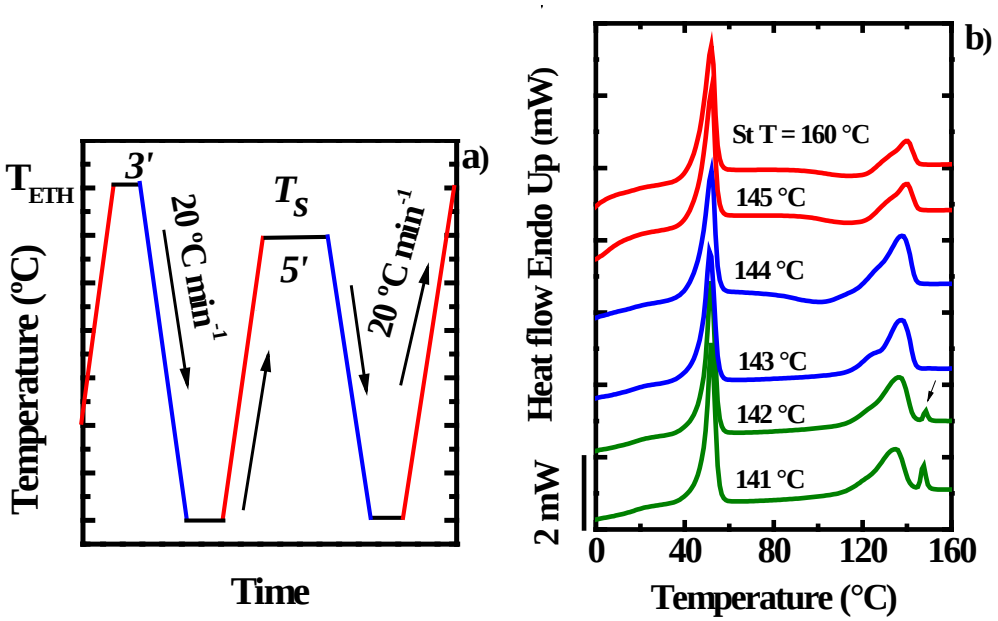

Figure 11. a) Self-nucleation (SN) thermal protocol. b) Subsequent DSC heating scans (A color code have been employed to indicate the self-nucleation domains: red for *Domain I*, blue for *Domain II* and green for *Domain III*).

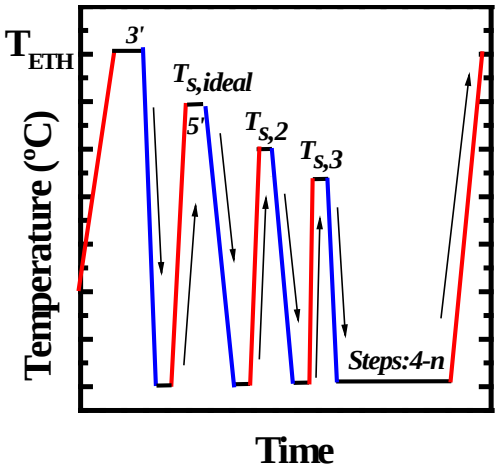

Figure 12. SSA thermal protocol schematic representation.

The sample selected was the $PCL_{43}PLLA_{57}^{15.4}$ diblock copolymer. **Figure 11b** shows the heating scan after the isothermal step at different T_s values (indicated in black for each curve). The characteristic annealing peaks at higher temperatures (signaled with an arrow in the green

curves, i.e., domain III) when 142 °C was used as self-nucleation temperature (T_s). Therefore, the ideal T_s temperature to apply the SSA protocol was 143 °C.

The SSA protocol consists of successive self-nucleation and annealing steps starting from $T_{s,ideal}$ (see **Figure 12**) until the full width of the melting range is covered. The difference between $T_{s,ideal}$ and the subsequent $T_{s,x}$ is usually 5 °C. This is the fractionation window and it should be kept constant throughout the SSA experiment.[77, 78] After several cycles, the sample is finally heated until complete melting. In this final step, the result of the SSA thermal fractionation is revealed.

Figure 13 depicts the final DSC heating scans of the PEO-*b*-PCL-*b*-PLLA triblock terpolymers, corresponding PCL-*b*-PLLA diblock copolymers and PLLA homopolymers after being subjected to the SSA treatment.

It is clear that the SSA treatment was effective in fractionating the PLLA block. These fractions are more evident in the triblock terpolymers and diblock copolymers with higher PLLA content, as expected. The series of melting peaks observed in both the PLLA range and the PEO/PCL range corresponds to the melting of crystals of different lamellar thickness created and annealed at each T_s.

Interestingly, the molten PEO and PCL chains contributes to enhance the lamellar thickness of the PLLA lamellae since the thermal fractions of this block melt at higher temperatures in comparison with PLLA homopolymer. This represents an additional evidence of the improved PLLA crystallizability caused by the PCL and PEO molten chains. What is more significant is that the SSA fractioning is able to clearly separate the melting peaks of the PCL and PEO blocks in the triblock terpolymers. Comparing to **Figure 10**, in which a double melting peak was observed in the range between 40 and 60 °C, after the SSA, the melting transitions of PEO and PCL are now well distinct (see **Figure 13c**), as the peaks above 50 °C are clearly due to the melting of PCL crystals (easily spotted by comparing diblock and triblock heating scans).

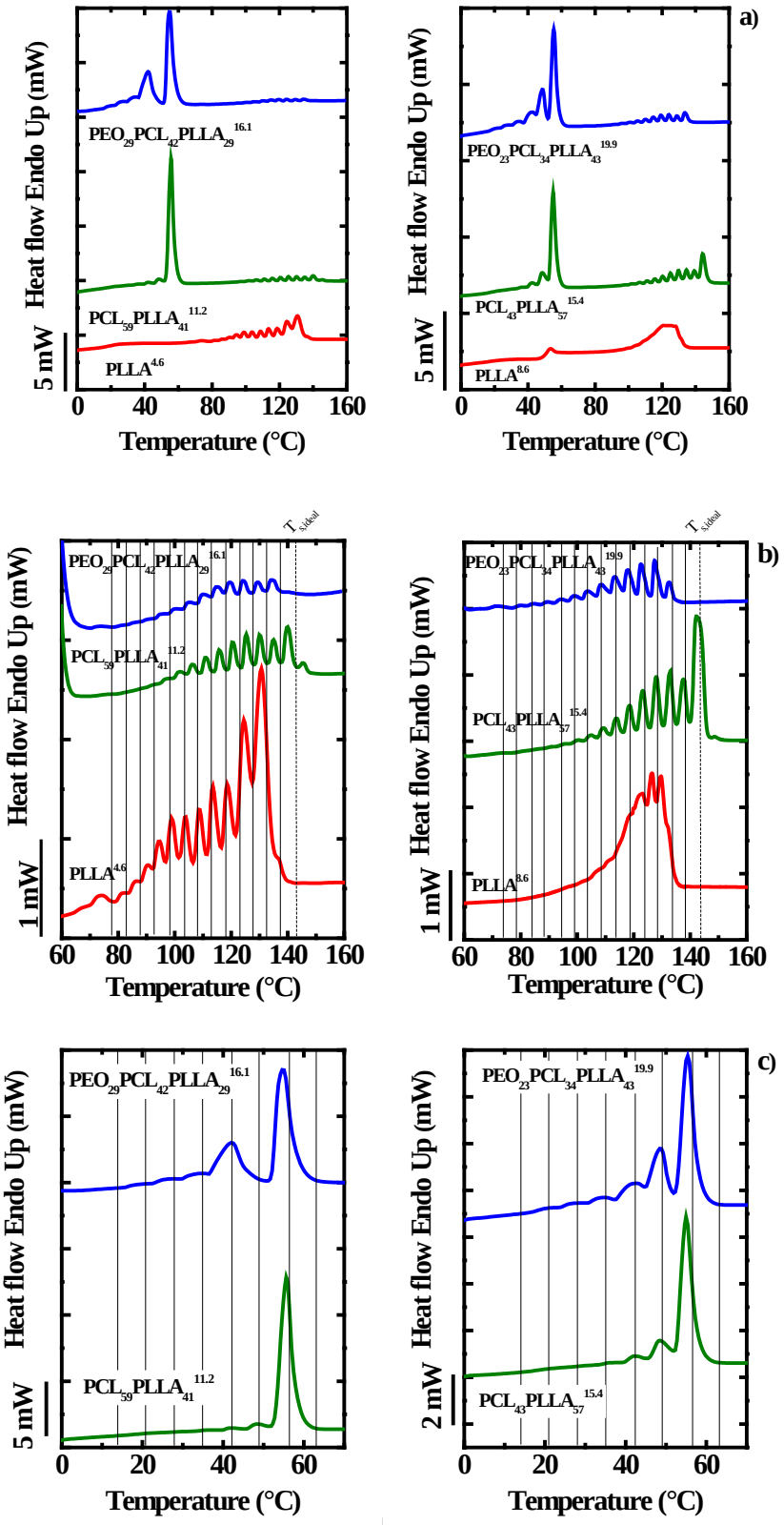

Figure 13. a) DSC heating scans at 20 °C.min^{-1} for the PEO-*b*-PCL-*b*-PLLA triblock terpolymers, PCL-*b*-PLLA diblock copolymers and PLLA homopolymers after the SSA thermal treatment. b) Zoom of the PLLA zone. c) Zoom of the PCL-PEO and PCL zone.

Which block melts first was again elucidated by WAXS analysis. **Figure 14** shows the WAXS patterns taken on heating of a SSA treated triblock terpolymer. It can be seen that the PEO reflection disappears first, indicating that PEO crystals are the first to melt upon heating, and after, the PCL block crystals. To sum up, the SSA technique was effective to properly fractionate the three blocks in triple crystalline PEO-*b*-PCL-*b*-PLLA triblock terpolymers.

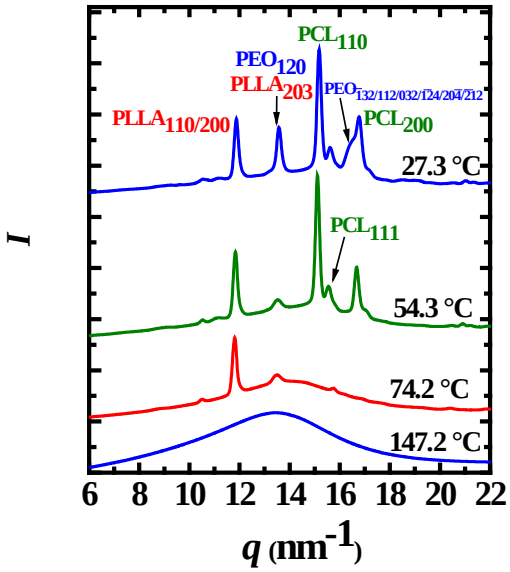

Figure 14. WAXS patterns of $PEO_{29}PCL_{42}PLLA_{29}^{16.1}$ taken at different temperatures during subsequent heating after SSA thermal treatment.

SSA is a versatile technique to thermally fractionate very complex systems, such as ABC triple crystalline triblock terpolymers. It can yield valuable information about the crystallization order in block copolymers and terpolymers, since it is very sensitive to any interruption of the chain that can limit its crystallization ability. Complementary analysis of the phase segregation employing SAXS techniques will be pursued in order to elucidate the structure of the phase segregation as a consequence of the SSA treatment.

9. Conclusions

In multicrystalline block copolymers, microphase separation driven by crystallization forces self-assemby into well-ordered lamellar nanostructures, depending on the crystallization conditions, composition and physical features of the blocks. These ordered nanostructures can be used in lithography, medical and optoelectronic devices. Additionally, multicrystalline block copolymers allow the study of the crystallization behavior at the nanoscale under confinement environment, and the crystallization analysis becomes more challenging as the number of potentially crystalline phases increases.

Particularly, the complexity of the crystallization behavior of PEO-*b*-PCL-*b*-PLLA triblock terpolymers with three crystallizable phases relies on different competitive effects that depend on the crystallization conditions and the particular physical properties of the blocks. In that sense, whether one of the phases is molten, amorphous or crystalline can affect the ability to crystallize of the other two, and as a result, complex opposite effects such as plasticization, nucleation, anti-plasticization and confinement might take place. Particularly, the PCL and PEO blocks caused a plasticizing effect over PLLA crystallization, while the PLLA phase could induce a nucleating effect over the PCL crystallization if this phase is crystallized, or an anti-plasticizing effect if this phase is amorphous. The PEO block crystallization is subjected to a hard confinement effect when the other two blocks are first crystallized. Thus, depending on the crystallization conditions, a trilamellar morphology can be tailored to tune the biodegradability of the material at the nanoscale. Moreover, SSA thermal fractionation is a suitable technique to thermally separate the three phases present in the triblock terpolymers.

The addition of a third crystallizable block to biodegradable diblock copolymers broadens the potential application of these biodegradable materials. Further analyses of the nucleation, crystallization and melting behavior, with novel techniques will be pursued. Surely, understanding the crystallization and self-assembly behavior of triple crystalline triblock terpolymers is expected to be in the focus of researchers for the next years.

10. Acknowledgements

The POLYMAT/UPV/EHU team would like to acknowledge funding from MINECO through project: MAT2017-83014-C2-1-P, and from ALBA synchrotron facility. We also acknowledge funding by the European Union´s Horizon 2020 research and innovation programme under the Marie Sklodowska-Curie grant agreement No 778092. The support of the National Key R&D Program of China (2017YFE0117800) is also gratefully acknowledged.

References

[1] C. M. Bates, F. S. Bates, *Macromolecules* **2017**, *50*, 3.
[2] I. W. Hamley, "Block Copolymers", in *Encyclopedia of Polymer Science and Technology*, John Wiley & Sons, Inc., 2002, p. 457.
[3] I. W. Hamley, "*The Physics of Block Copolymers*", Oxford University Press, Oxford 1998.
[4] N. Hadjichristidis, M. Pitsikalis, H. Iatrou, *Adv. Polym. Sci.* **2005**, *189*, 1.
[5] S. Huang, S. Jiang, *RSC Advances* **2014**, *4*, 24566.
[6] M. J. Barthel, F. H. Schacher, U. S. Schubert, *Polym. Chem.* **2014**, *5*, 2647.
[7] X. Guo, L. Wang, X. Wei, S. Zhou, *Journal of Polymer Science, Part A: Polymer Chemistry* **2016**, *54*, 3525.
[8] H. Danafar, *Drug Research* **2016**, *66*, 506.
[9] L. Zha, W. Hu, *Prog. Polym. Sci.* **2016**, *54-55*, 232.
[10] S. Nakagawa, H. Marubayashi, S. Nojima, *Eur. Polym. J.* **2015**, *70*, 262.
[11] W. N. He, J. T. Xu, *Prog. Polym. Sci.* **2012**, *37*, 1350.
[12] C. Yu, Q. Xie, Y. Bao, G. Shan, P. Pan, *Crystals* **2017**, *7*, 147.
[13] R. M. Michell, A. J. Müller, *Prog. Polym. Sci.* **2016**, *54-55*, 183.
[14] A. J. Müller, M. L. Arnal, A. T. Lorenzo, "Crystallization in Nano-Confined Polymeric Systems", in *Handbook of Polymer Crystallization*, E. Piorkowska and G.C. Rutledge, Eds., John Wiley and Sons, Hoboken, New Jersey, 2013, p. 347.
[15] H. Takeshita, T. Shiomi, K. Takenaka, F. Arai, *Polymer* **2013**, *54*, 4776.
[16] S. Li, R. A. Register, "Crystallization in Copolymers ", in *Handbook of Polymer Crystallization*, E. Piorkowska and G.C. Rutledge, Eds., John Wiley and Sons, Hoboken, New Jersey, 2013, p. 327.
[17] R. V. Castillo, A. J. Müller, *Prog. Polym. Sci.* **2009**, *34*, 516.
[18] A. J. Müller, M. L. Arnal, V. Balsamo, *Lecture Notes in Physics* **2007**, *714*, 229.
[19] A. J. Müller, V. Balsamo, M. L. Arnal, *Adv. Polym. Sci.* **2005**, *190*, 1.
[20] V. Abetz, P. F. W. Simon, *Adv. Polym. Sci.* **2005**, *189*, 125.
[21] I. Hamley, *Adv. Polym. Sci.* **1999**, *148*, 113.
[22] R. M. Van Horn, M. R. Steffen, D. O'Connor, *POLYMER CRYSTALLIZATION* **2018**, *1*, e10039.
[23] Y. L. Loo, R. A. Register, A. J. Ryan, *Macromolecules* **2002**, *35*, 2365.
[24] H. Ge, F. J. Zhang, H. Y. Huang, T. B. He, *Acta Polymerica Sinica* **2019**, *50*, 82.
[25] M. Ponjavic, M. S. Nikolic, S. Jevtic, J. Rogan, S. Stevanovic, J. Djonlagic, *Macromolecular Research* **2016**, *24*, 323.
[26] Y. Li, J. Zhou, J. Zhang, Q. Gou, Q. Gu, Z. Wang, *Journal of Macromolecular Science, Part B: Physics* **2014**, *53*, 1137.
[27] Y. Li, H. Huang, Z. Wang, T. He, *Macromolecules* **2014**, *47*, 1783.
[28] F. F. Xue, X. S. Chen, L. J. An, S. S. Funari, S. C. Jiang, *Chinese Journal of Polymer Science (English Edition)* **2013**, *31*, 1260.
[29] F. Xue, X. Chen, L. An, S. S. Funari, S. Jiang, *Polym. Int.* **2012**, *61*, 909.
[30] J. Sun, C. He, X. Zhuang, X. Jing, X. Chen, *J. Polym. Res.* **2011**, *18*, 2161.
[31] R. M. Van Horn, J. X. Zheng, H. J. Sun, M. S. Hsiao, W. B. Zhang, X. H. Dong, J. Xu, E. L. Thomas, B. Lotz, S. Z. D. Cheng, *Macromolecules* **2010**, *43*, 6113.
[32] L. Li, F. Meng, Z. Zhong, D. Byelov, W. H. De Jeu, J. Feijen, *J. Chem. Phys.* **2007**, *126*.
[33] C. Hua, C.-M. Dong, *Journal of Biomedical Materials Research Part A* **2007**, *82A*, 689.
[34] M. Vivas, J. Contreras, F. López-Carrasquero, A. T. Lorenzo, M. L. Arnal, V. Balsamo, A. J. Müller, E. Laredo, H. Schmalz, V. Abetz, *Macromol. Sym.* **2006**, *239*, 58.
[35] C. He, J. Sun, T. Zhao, Z. Hong, X. Zhuang, X. Chen, X. Jing, *Biomacromolecules* **2006**, *7*, 252.
[36] S. Jiang, C. He, L. An, X. Chen, B. Jiang, *Macromol. Chem. Phys.* **2004**, *205*, 2229.
[37] M. L. Arnal, F. López-Carrasquero, E. Laredo, A. J. Müller, *Eur. Polym. J.* **2004**, *40*, 1461.
[38] L. Piao, Z. Dai, M. Deng, X. Chen, X. Jing, *Polymer* **2003**, *44*, 2025.
[39] M. L. Arnal, V. Balsamo, F. López-Carrasquero, J. Contreras, M. Carrillo, H. Schmalz, V. Abetz, E. Laredo, A. J. Müller, *Macromolecules* **2001**, *34*, 7973.
[40] B. Bogdanov, A. Vidts, A. Van Den Buicke, R. Verbeeck, E. Schacht, *Polymer* **1998**, *39*, 1631.
[41] S. Nojima, M. Ono, T. Ashida, *Polym. J.* **1992**, *24*, 1271.
[42] Z. Wei, L. Liu, F. Yu, P. Wang, M. Qi, *J. Appl. Polym. Sci.* **2009**, *111*, 429.
[43] Z. Wei, F. Yu, G. Chen, C. Qu, P. Wang, W. Zhang, J. Liang, M. Qi, L. Liu, *J. Appl. Polym. Sci.* **2009**, *114*, 1133.
[44] M. L. Arnal, S. Boissé, A. J. Müller, F. Meyer, J. M. Raquez, P. Dubois, R. E. Prud'Homme, *CrystEngComm* **2016**, *18*, 3635.
[45] D. Zhou, J. Sun, J. Shao, X. Bian, S. Huang, G. Li, X. Chen, *Polymer* **2015**, *80*, 123.
[46] J. Yang, Y. Liang, C. C. Han, *Polymer (United Kingdom)* **2015**, *79*, 56.

[47] F. Xue, X. Chen, L. An, S. S. Funari, S. Jiang, *RSC Advances* **2014**, *4*, 56346.
[48] S. Huang, H. Li, S. Jiang, X. Chen, L. An, *Polym. Bull.* **2011**, *67*, 885.
[49] S. Huang, S. Jiang, L. An, X. Chen, *J. Polym. Sci., Part B: Polym. Phys.* **2008**, *46*, 1400.
[50] J. Yang, T. Zhao, Y. Zhou, L. Liu, G. Li, E. Zhou, X. Chen, *Macromolecules* **2007**, *40*, 2791.
[51] C. Cai, L. U. Wang, C. M. Donc, *J. Polym. Sci., Part A: Polym. Chem.* **2006**, *44*, 2034.
[52] J. Yang, T. Zhao, J. Cui, L. Liu, Y. Zhou, G. Li, E. Zhou, X. Chen, *J. Polym. Sci., Part B: Polym. Phys.* **2006**, *44*, 3215.
[53] C. G. Mothé, W. S. Drumond, S. H. Wang, *Thermochim. Acta* **2006**, *445*, 61.
[54] C. I. Huang, S. H. Tsai, C. M. Chen, *J. Polym. Sci., Part B: Polym. Phys.* **2006**, *44*, 2438.
[55] D. Shin, K. Shin, K. A. Aamer, G. N. Tew, T. P. Russell, J. H. Lee, J. Y. Jho, *Macromolecules* **2005**, *38*, 104.
[56] J. Sun, Z. Hong, L. Yang, Z. Tang, X. Chen, X. Jing, *Polymer* **2004**, *45*, 5969.
[57] K. S. Kim, S. Chung, I. J. Chin, M. N. Kim, J. S. Yoon, *J. Appl. Polym. Sci.* **1999**, *72*, 341.
[58] R. Liénard, N. Zaldua, T. Josse, J. D. Winter, M. Zubitur, A. Mugica, A. Iturrospe, A. Arbe, O. Coulembier, A. J. Müller, *Macromol. Rapid Commun.* **2016**, *37*, 1676.
[59] I. Navarro-Baena, A. Marcos-Fernández, A. Fernández-Torres, J. M. Kenny, L. Peponi, *RSC Advances* **2014**, *4*, 8510.
[60] L. Peponi, I. Navarro-Baena, J. E. Báez, J. M. Kenny, A. Marcos-Fernández, *Polymer* **2012**, *53*, 4561.
[61] D. Yan, H. Huang, T. He, F. Zhang, *Langmuir* **2011**, *27*, 11973.
[62] M. T. Casas, J. Puiggalí, J. M. Raquez, P. Dubois, M. E. Córdova, A. J. Müller, *Polymer* **2011**, *52*, 5166.
[63] R. V. Castillo, A. J. Müller, J. M. Raquez, P. Dubois, *Macromolecules* **2010**, *43*, 4149.
[64] J. L. Wang, C. M. Dong, *Macromol. Chem. Phys.* **2006**, *207*, 554.
[65] I. W. Hamley, P. Parras, V. Castelletto, R. V. Castillo, A. J. Müller, E. Pollet, P. Dubois, C. M. Martin, *Macromol. Chem. Phys.* **2006**, *207*, 941.
[66] I. W. Hamley, V. Castelletto, R. V. Castillo, A. J. Müller, C. M. Martin, E. Pollet, P. Dubois, *Macromolecules* **2005**, *38*, 463.
[67] O. Jeon, S. H. Lee, S. H. Kim, Y. M. Lee, Y. H. Kim, *Macromolecules* **2003**, *36*, 5585.
[68] R. M. Ho, P. Y. Hsieh, W. H. Tseng, C. C. Lin, B. H. Huang, B. Lotz, *Macromolecules* **2003**, *36*, 9085.
[69] V. Tamboli, G. P. Mishra, A. K. Mitra, *Colloid. Polym. Sci.* **2013**, *291*, 1235.
[70] Y.-W. Chiang, Y.-Y. Hu, J.-N. Li, S.-H. Huang, S.-W. Kuo, *Macromolecules* **2015**, *48*, 8526.
[71] J. K. Palacios, A. Mugica, M. Zubitur, A. Iturrospe, A. Arbe, G. Liu, D. Wang, J. Zhao, N. Hadjichristidis, A. J. Muller, *RSC Advances* **2016**, *6*, 4739.
[72] L. Sun, L. J. Shen, M. Q. Zhu, C. M. Dong, Y. Wei, *J. Polym. Sci., Part A: Polym. Chem.* **2010**, *48*, 4583.
[73] J. K. Palacios, A. Mugica, M. Zubitur, A. J. Müller, "Crystallization and morphology of block copolymers and terpolymers with more than one crystallizable block", in *Crystallization in Multiphase Polymer Systems*, 2018, p. 123.
[74] J. K. Palacios, A. Tercjak, G. Liu, D. Wang, J. Zhao, N. Hadjichristidis, A. J. Müller, *Macromolecules* **2017**, *50*, 7268.
[75] J. K. Palacios, J. Zhao, N. Hadjichristidis, A. J. Müller, *Macromolecules* **2017**, *50*, 9683.
[76] A. J. Müller, M. Avila, G. Saenz, J. Salazar, "Crystallization of PLA-based Materials", in *Poly(lactic acid) Science and Technology: Processing, Properties, Additives and Applications*, A. Jimenez, M. Peltzer, and R. Ruseckaite, Eds., The Royal Society of Chemistry, Cambridge, 2015, p. 66.
[77] A. J. Müller, M. L. Arnal, *Prog. Polym. Sci.* **2005**, *30*, 559.
[78] A. J. Müller, R. M. Michell, R. A. Pérez, A. T. Lorenzo, *Eur. Polym. J.* **2015**, *65*, 132.
[79] H. Alamri, J. Zhao, D. Pahovnik, N. Hadjichristidis, *Polym. Chem.* **2014**, *5*, 5471.
[80] J. Zhao, D. Pahovnik, Y. Gnanou, N. Hadjichristidis, *Polym. Chem.* **2014**, *5*, 3750.
[81] M. Rubinstein, R. H. Colby, "*Polymer Physics*", OUP Oxford, 2003.
[82] C. He, J. Sun, J. Ma, X. Chen, X. Jing, *Biomacromolecules* **2006**, *7*, 3482.
[83] Y.-W. Chiang, Y.-Y. Hu, J.-N. Li, S.-H. Huang, S.-W. Kuo, "Trilayered Single Crystals with Epitaxial Growth in Poly(ethylene oxide)-block-poly(ε-caprolactone)-block-poly(l-lactide) Thin Films", in *Macromolecules*, American Chemical Society, 2015.
[84] P. Pan, W. Kai, B. Zhu, T. Dong, Y. Inoue, *Macromolecules* **2007**, *40*, 6898.
[85] J. R. Sarasua, R. E. Prud'homme, M. Wisniewski, A. Le Borgne, N. Spassky, *Macromolecules* **1998**, *31*, 3895.
[86] Y. Wang, J. F. Mano, *Eur. Polym. J.* **2005**, *41*, 2335.
[87] M. L. Di Lorenzo, *J. Appl. Polym. Sci.* **2006**, *100*, 3145.

(1)

New generation of triple crystalline ABC triblock terpolymers composed of PEO, PCL and PLLA (PEO-*b*-PCL-*b*-PLLA). The remarkable tricrystalline structure and the complex crystallization behavior of these materials are discussed. New insights on the intricate interplay between the blocks are presented by means of Successive Self-nucleation and Annealing (SSA) thermal fractionation.

Keyword: triblock terpolymers, diblock copolymers, polymer crystallization.

Jordana K. Palacios, Guoming Liu, Dujin Wang, Nikos Hadjichristidis* and Alejandro J. Müller*

Title

Generating Triple Crystalline Superstructures in Melt Miscible PEO-*b*-PCL-*b*-PLLA Triblock Terpolymers by Controlling Thermal History and Sequential Crystallization